

Chapter 10

Heat Transfer Study for ADS Solid Target: Surface Wettability and Its Effect on a Boiling Heat Transfer

Daisuke Ito, Kazuki Hase, and Yasushi Saito

Abstract In relationship to a solid target cooling system of an accelerator-driven system (ADS), wettability effect on boiling heat transfer has been experimentally investigated by irradiation with ultraviolet and gamma rays (γ -rays). The experimental apparatus consists of a copper heater block, a rectangular container, and a thermostat bath. Two copper heater blocks were fabricated: one is for radiation-induced surface activation (RISA) and the other is for photoelectric reaction by ultraviolet whose heat transfer surface is coated by a TiO_2 film. These copper heater blocks were irradiated by ultraviolet or by γ -rays to change the surface wettability. Boiling heat transfer under subcooling conditions was measured before and after the irradiations to study the wettability effect. Experimental results show that nucleate boiling curves are shifted to the higher wall superheated side with the irradiated surface because of the decrease of the active nucleation sites. Heat transfer enhancement was found in both the critical heat flux and microbubble emission boiling (MEB) regions under these experimental conditions.

Keywords Microbubble emission boiling • Photocatalysis • Proton beam • Radiation-induced surface activation • Surface wettability

10.1 Introduction

An accelerator-driven system (ADS) is a hybrid-type nuclear system consisting of a proton accelerator, a spallation target, and a subcritical assembly in which high-energy particles and high heat density are generated in the target and subcritical assembly by the spallation and fission reactions. Lead-bismuth is considered the leading candidate for the liquid-metal spallation target for nuclear transmutation

D. Ito (✉) • Y. Saito
Research Reactor Institute, Kyoto University, 2-1010 Asashiro-nishi,
Kumatori-cho, Sennan-gun, Osaka 590-0494, Japan
e-mail: itod@rri.kyoto-u.ac.jp

K. Hase
Power Systems Company, Toshiba Corporation, Kawasaki, Japan

[1–3], whereas a solid target such as tungsten or tantalum should be also developed for a water-cooled ADS neutron source [4, 5].

High-energy radiation affects the surface wettability and boiling heat transfer of the solid target. Wettability on a solid surface can be changed by using ultraviolet radiation or γ -rays, and recently the authors have found that the surface wettability can be also changed by proton-beam irradiation [6]. Applying the wettability change resulting from ultraviolet irradiation to titanium dioxide (TiO_2), heat transfer research has been carried out to evaluate the wettability effect [7]. In addition, radiation-induced surface activation (RISA) enhances the surface wettability by irradiating a metal oxide layer with γ -rays. Takamasa et al. [8] have applied RISA to heat-transfer experiments and reported that boiling heat transfer could be enhanced by changing the wettability of the heating surface. However, there has been no research to investigate surface wettability effect on boiling heat transfer at a solid target cooling system, where microbubble emission boiling (MEB) [9] might occur. MEB can take place when the heat transfer area is small (about 1 cm^2) with subcooling conditions. In the target cooling system, the target should be cooled by subcooled water, and the heat-transfer area can be small when the proton beam is focused to a small area. Thus, MEB should be investigated for thermal hydraulic design and safety analysis of the solid target system, and also the effect of wettability on boiling heat transfer should be studied.

The purpose of this study is to investigate wettability change by ultraviolet, γ -ray, and proton beam and to study the wettability effect on subcooled boiling heat transfer with a small heat-transfer area, and finally to obtain knowledge on the heat-transfer mechanism of the MEB phenomena.

10.2 Surface Wettability Change by Irradiation

10.2.1 *Sample and Irradiation Facility*

To investigate surface wettability change by irradiation, samples are irradiated by using an ultraviolet lamp, a ^{60}Co γ -ray source, and a proton accelerator. In this study, a TiO_2 sample, which is a typical photocatalyst [10], is used to compare the irradiation effects of ultraviolet, γ -ray, and proton beam. TiO_2 is prepared through anodizing a 0.1-mm-thick titanium plate [11]. Details of the experimental procedure with TiO_2 samples and irradiation facilities are described as follows.

10.2.1.1 Ultraviolet

Ultraviolet irradiates TiO_2 by using a commercial UV lamp. Irradiation intensity is measured by an ultraviolet meter and is controlled by changing the distance between the lamp and the sample. The intensity is varied at a range from 0.01

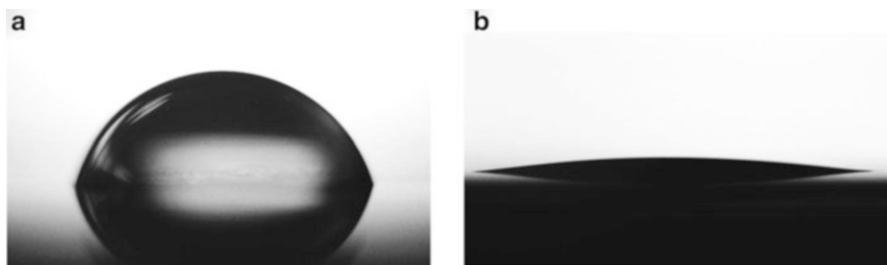


Fig. 10.1 Water droplets on the TiO_2 surface before and after ultraviolet irradiation. (a) Before ultraviolet irradiation. (b) After ultraviolet irradiation with 1 mW/cm^2 for 1 h

to 5 mW/cm^2 . The center wavelength of the ultraviolet from this lamp is 365 nm. Figure 10.1 shows a typical irradiation effect on surface wettability change before and after ultraviolet irradiation.

10.2.1.2 Gamma Rays (γ -Rays)

The ^{60}Co γ -ray irradiation facility in the Research Reactor Institute, Kyoto University, is utilized for γ -ray irradiation. The integrated irradiation dose is estimated by an irradiation time and a distance from the γ -ray source. The γ -ray energy of this facility is about 1 MeV (1.17 and 1.33 MeV) and the maximum dose rate is about 15 kGy/h.

10.2.1.3 Proton Beam

The FFAG (fixed-field alternating gradient) accelerator in the Research Reactor Institute, Kyoto University, is utilized for proton-beam irradiation. The energy of the proton beam is set at about 100 or 150 MeV. The maximum beam current of this facility is about 10 nA.

10.2.2 Contact Angle Measurement

The wettability of the sample before and after irradiation is evaluated by measuring the contact angle of a water droplet on a sample surface. The measurement system (Fig. 10.2) consists of a digital video camera, a stage (with a biaxial stage and a goniometer), a backlight, and a PC. Pure water of $2 \mu\text{l}$ is dropped onto the horizontal surface of the sample using a micropipette. The water droplet is imaged by the camera and the images are processed to obtain the contact angle. In the image processing, it is assumed that the droplet is a part of a sphere (Fig. 10.3), and the contact angle is estimated by the following equation:

Fig. 10.2 Contact angle measurement system

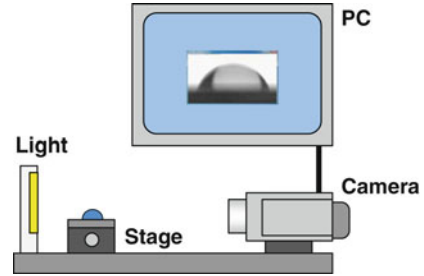
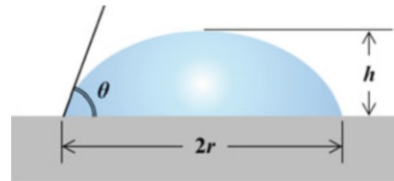


Fig. 10.3 Estimation of contact angle



$$\theta = \sin^{-1} \frac{2rh}{r^2 + h^2} \quad (10.1)$$

where r and h are obtained by using an image processing software (ImageJ).

10.2.3 Effect of Irradiations on Surface Wettability

Figure 10.4a–c shows the wettability change from ultraviolet, γ -ray, and proton-beam irradiation, respectively. The horizontal axis denotes an integrated irradiation dose or irradiation time and the vertical axis denotes the measured contact angle. As shown in these figures, the contact angle decreases with the irradiation dose. In these experiments, the ambient effect is also studied during the irradiations, which are performed in air or water. As shown in Fig. 10.4a, the ambient effect on the contact angle change is not obvious in the ultraviolet irradiation. However, the ambient effect is very distinct both in the γ -ray and the proton-beam irradiations. It is suggested that the wettability enhancement by the radiations may be attributed to the radiolysis of water.

10.3 Effect of Boiling Heat Transfer on Surface Wettability

10.3.1 Experimental Setup and Procedure

A schematic view of the experimental apparatus for pool boiling experiments with small heat transfer area is shown in Fig. 10.5. The apparatus consists of a copper block, a furnace, a rectangular container, and a heat exchanger. The copper block has a cylindrical part (10 mm in diameter, 15 mm in height). Several cartridge

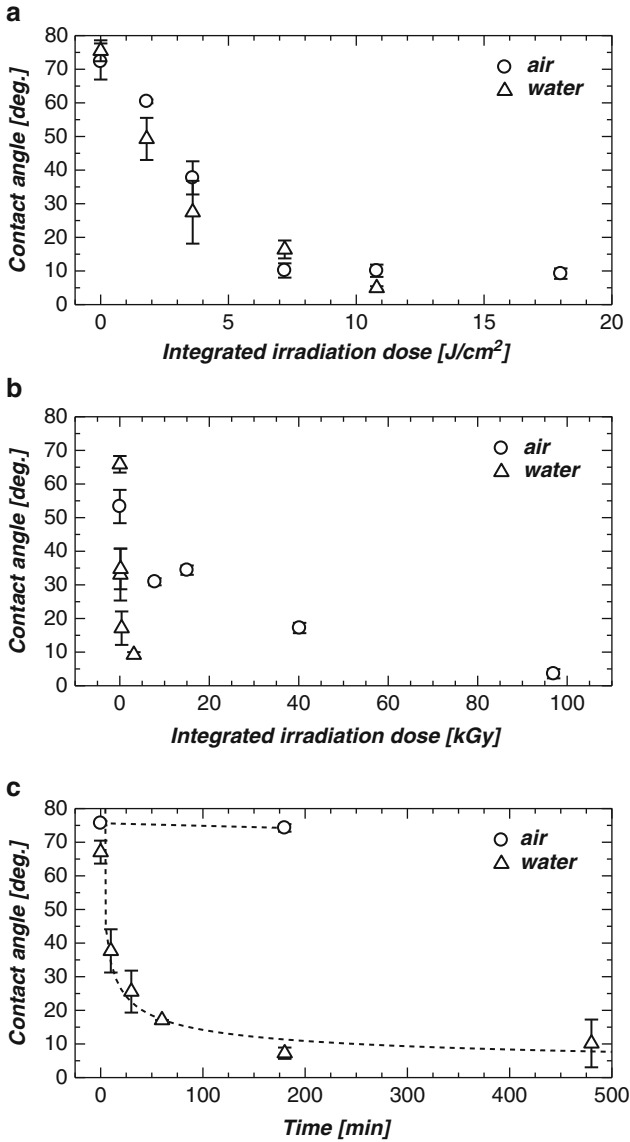


Fig. 10.4 Change of contact angle from ultraviolet, γ -ray, and proton beam irradiation to TiO_2 sample. (a) Ultraviolet irradiation. (b) γ -Ray irradiation. (c) Proton beam irradiation

heaters are installed in the copper block (3 kW in total). Two different copper blocks were fabricated to investigate the wettability effect on the heat transfer: one is a test section for ultraviolet irradiation and the other is for γ -ray irradiation. Both test sections are illustrated in Fig. 10.5: three thermocouples are inserted into the cylindrical part of each copper block to estimate heat flux and surface temperature.

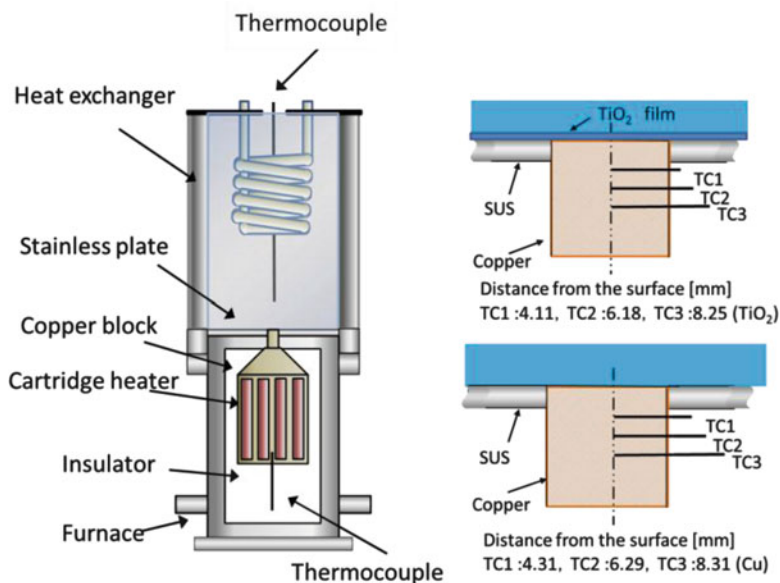


Fig. 10.5 Schematic of experimental apparatus

Table 10.1 Irradiation conditions

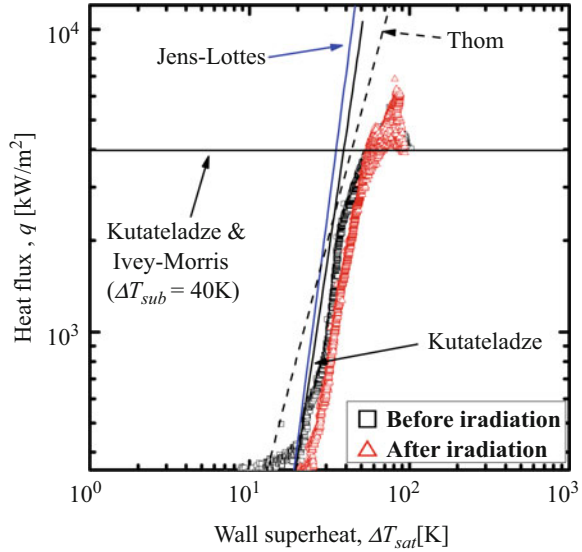
| | | |
|-----------------------|-------------------------------|---------------|
| Irradiation source | Ultraviolet | γ -ray |
| Surface material | TiO ₂ | Copper oxide |
| Irradiation condition | 3 mW/cm ² , 30 min | 220 kGy |

The heat transfer surface for ultraviolet experiments is coated by a TiO₂ thin film by a sputtering process in Kyushu University. The surface for γ -ray experiments is polished with #400 emery paper and then heated in air at 200 °C for 1 h. After the thermal oxidation of the copper surface, it is irradiated in the ⁶⁰Co facility where the integrated dose is 220 kGy. The irradiation conditions for heat-transfer experiments are summarized in Table 10.1.

10.3.2 Results and Discussion

Measured boiling curves with and without ultraviolet irradiation are shown in Fig. 10.6. Calculated lines denote existing correlations for nucleate boiling [12–14] and critical heat flux [15, 16]. As shown in this figure, the boiling curve after irradiation moves to the higher wall superheated side in the nucleate boiling region, which may be caused by inactivation of nucleation sites on the heat transfer surface resulting from hydrophilicity. In this experiment the maximum heat flux after the

Fig. 10.6 Boiling curve before and after ultraviolet irradiation



nucleate boiling region is defined as a critical heat flux (CHF). In both boiling curves, the wall temperature rises rapidly just after the CHF region and the heat flux increases with decreasing wall temperature, resulting in heat flux being larger than CHF. These phenomena can be considered as a microbubble emission boiling (MEB) because many small bubbles are observed in this region. In the MEB region the boiling curve after irradiation moves to the lower wall superheated side, in contrast to the nucleate boiling region.

Measured boiling curves with and without γ -ray irradiation are shown in Figs. 10.7, 10.8, and 10.9. Table 10.2 shows the contact angles before and after irradiation to the oxidized copper surface. As shown in these figures, MEB phenomena are observed with or without irradiation for $\Delta T_{sub} = 20, 40, \text{ and } 60 \text{ K}$. The boiling curves in the nucleate boiling region (low superheat region) are shifted to the higher superheat side similar to the ultraviolet irradiation experiments. However, in contrast, the boiling curves in the MEB region (higher superheat region) are shifted to the lower superheat side after irradiation, which may be caused by enhancement of thin liquid film at the re-wetting phenomena.

CHF and maximum heat fluxes in the MEB region are plotted against liquid subcooling in Fig. 10.10. Solid and dashed lines denote the predicted values of existing CHF correlations by Kutateladze [15] and Haramura and Katto [17], respectively. The measured CHF agree well with the predicted values by the aforementioned existing correlations. Measured CHF after the irradiations are slightly larger than those before the irradiations; however, the effect of the irradiation on the CHF is not obvious in the present experimental conditions. Maximum heat flux in the MEB region is almost 50 % larger than the CHF value, and the effect of the irradiation on the maximum heat flux is also not distinct, similar to the CHF within present experimental conditions.

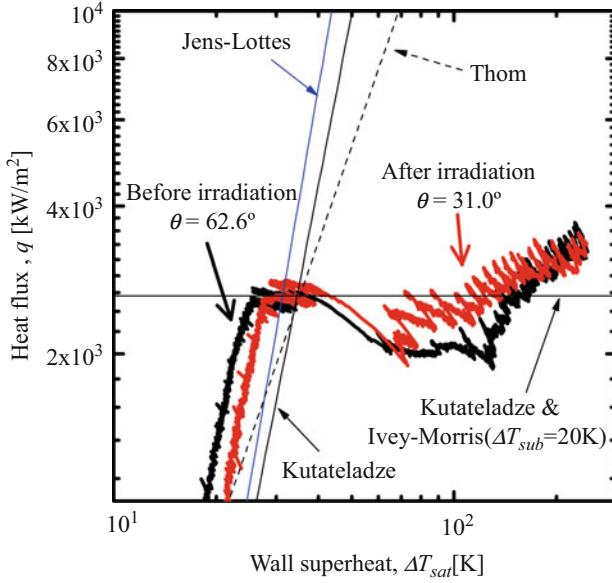


Fig. 10.7 Boiling curve before and after γ -ray for $\Delta T_{sub} = 20$ K

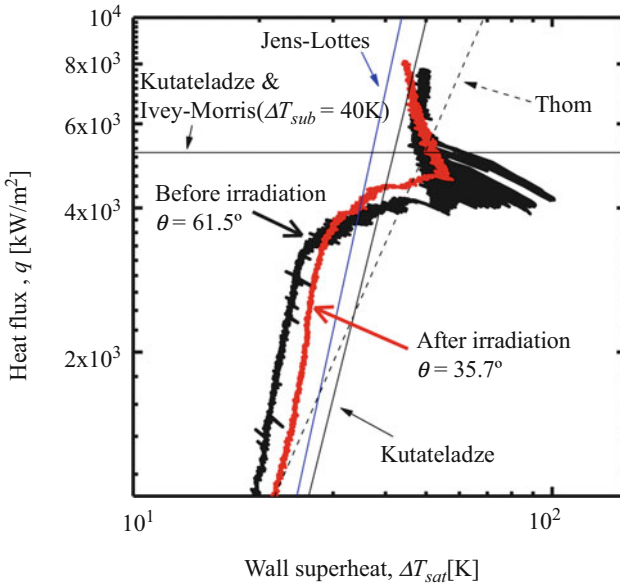


Fig. 10.8 Boiling curve before and after γ -ray for $\Delta T_{sub} = 40$ K

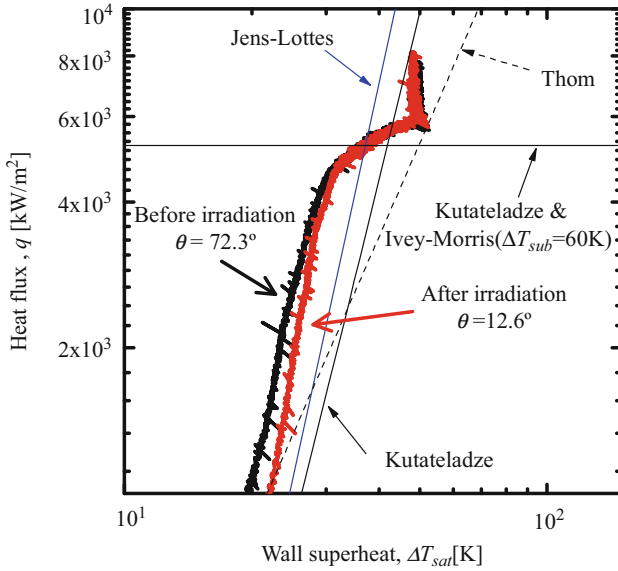
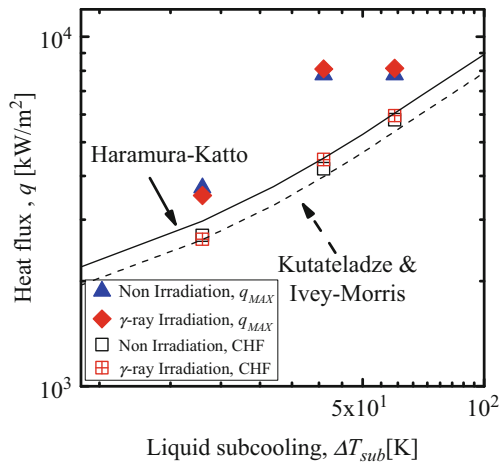


Fig. 10.9 Boiling curve before and after γ -ray for $\Delta T_{sub} = 60$ K

Table 10.2 Contact angles before and after γ -ray irradiations

| Subcooling (K) | Before irradiation ($^\circ$) | After irradiation ($^\circ$) |
|----------------|---------------------------------|--------------------------------|
| 20 | 62.6 | 31.0 |
| 40 | 61.5 | 35.7 |
| 60 | 72.3 | 12.6 |

Fig. 10.10 Critical heat flux (CHF) and maximum heat flux before and after γ -ray irradiation



10.4 Conclusions

Effect of surface wettability on boiling heat transfer was studied by applying photocatalysis effect and radiation-induced surface activation. The main conclusions are as follows.

- Wettability enhancement was observed by proton-beam irradiation as well as the ultraviolet and γ -ray irradiation.
- In comparing the irradiation between that in air and that in water, no influence of the radiation environment is observed for ultraviolet irradiation. However, the wettability was well enhanced by γ -ray and proton-beam irradiation in water rather than in air.
- The boiling curve with ultraviolet irradiation moves to the higher wall superheated side in the nucleate boiling region. In contrast, the boiling curve with irradiation moves to the lower wall superheated side in the MEB region.
- A similar tendency of the boiling curve was observed with γ -ray irradiation in comparison to the ultraviolet irradiation.
- The effect of irradiation on the CHF was not obvious at present experimental conditions.

Acknowledgments The authors express their sincere gratitude to Prof. Y. Takata and Dr. S. Hidaka of Kyushu University for their valuable comments and technical assistance. A part of this study is the result of “Research and Development for an Accelerator-Driven Sub-Critical System using a FFAG Accelerator” carried out under the Strategic Promotion Program for Basic Nuclear Research by the Ministry of Education, Culture, Sports, Science and Technology of Japan.

Open Access This chapter is distributed under the terms of the Creative Commons Attribution Noncommercial License, which permits any noncommercial use, distribution, and reproduction in any medium, provided the original author(s) and source are credited.

References

1. Cinotti L, Giraud B, Ait Abderrahim H (2004) The experimental accelerator driven system (XADS) designs in the EURATOM 5th framework programme. *J Nucl Mater* 335:148–155
2. Maes D (2006) Mechanical design of the small-scale experimental ADS: MYRRHA. *Energ Convers Manag* 47:2710–2723
3. Oigawa H et al (2011) Role of ADS in the back-end of the fuel cycle strategies and associated design activities: the case of Japan. *J Nucl Mater* 415:229–236
4. Cheng X et al (2006) Thermal-hydraulic analysis of the TRADE spallation target. *Nucl Instrum Methods Phys Res A* 562:855–858
5. Hao J-H et al (2013) Target thickness optimization design of a spallation neutron source target cooling system. *Appl Therm Eng* 61:641–648
6. Ito D, Nishi D, Saito Y (2014) Effect of ultraviolet and radiation on surface wettability. *Multiphase Flow* 30:209–220 (in Japanese)

7. Takata Y, Hidaka S, Cao JM, Nakamura T, Yamamoto H, Masuda M, Ito T (2005) Effect of surface wettability on boiling and evaporation. *Energy* 30:209–220
8. Takamasa T, Hazuku T, Okamoto K, Mishima K, Furuya M (2005) Radiation-induced surface activation on Leidenfrost and quenching phenomena. *Exp Therm Fluid Sci* 29:267–274
9. Suzuki K et al (2005) Enhancement of heat transfer in subcooled flow boiling with microbubble emission. *Exp Therm Fluid Sci* 29:827–832
10. Fujishima A, Honda K (1972) Electrochemical photolysis of water at a semiconductor electrode. *Nature (Lond)* 238:37–38
11. Masahashi N, Semboshi S, Ohtsu N, Oku M (2008) Microstructure and superhydrophilicity of anodic TiO₂ films on pure titanium. *Thin Solid Films* 516:7488–7496
12. Kutateladze SS (1952) Heat transfer in condensation and boiling, 2nd edn. AEC-trans-3770. U.S. Atomic Energy Commission, Technical Information Service, Washington
13. Jens WH, Lottes PA (1962) Analysis of heat transfer, burnout, pressure drop and density data for high pressure water. USAEC Report ANL-4627
14. Thom JRS, Walker WM, Fallon TA, Reising GFS (1966) Boiling in subcooled water during flow up heated tubes or annuli. *Proc Inst Mech Eng* 180:226–246, Part 3C
15. Kutateladze SS (1953) Heat transfer in condensation and boiling, 2nd edn. AEC-trans-3405, U. S. AEC Technical Information Service,
16. Ivey HJ, Morris DJ (1962) On the relevance of the vapor-liquid exchange mechanism for subcooled boiling heat transfer at high pressure. AEEW Report 137, UKAEA
17. Haramura Y, Katto Y (1983) A new hydrodynamic model of critical heat flux, applicable widely to both pool and forced convection boiling on submerged bodies in saturated liquids. *Int J Heat Mass Transfer* 26-3:389–399